Article

Studies on the Kinetics of the CH + H$_2$ Reaction and Implications for the Reverse Reaction, ^{3}CH$_2$ + H

Published as part of The Journal of Physical Chemistry virtual special issue "Combustion in a Sustainable World: From Molecules to Processes".

Mark A. Blitz,* Lavinia Onel, Struan H. Robertson, and Paul W. Seakins*

ACCESS | Metrics & More | Article Recommendations | SI Supporting Information

ABSTRACT: The reaction of CH radicals with H$_2$ has been studied by the use of laser flash photolysis, probing CH decays under pseudo-first-order conditions using laser-induced fluorescence (LIF) over the temperature range 298−748 K at pressures of ∼5−100 Torr. Careful data analysis was required to separate the CH LIF signal at ∼428 nm from broad background fluorescence, and this interference increased with temperature. We believe that this interference may have been the source of anomalous pressure behavior reported previously in the literature (Brownsword, R. A.; et al. *J. Chem. Phys.* **1997**, *106*, 7662−7677). The rate coefficient k_1 shows complex behavior: at low pressures, the main route for the CH$_3$* formed from the insertion of CH into H$_2$ is the formation of ^{3}CH$_2$ + H, and as the pressure is increased, CH$_3$* is increasingly stabilized to CH$_3$. The kinetic data on CH + H$_2$ have been combined with experimental shock tube data on methyl decomposition and literature thermochemistry within a master equation program to precisely determine the rate coefficient of the reverse reaction, ^{3}CH$_2$ + H → CH + H$_2$. The resulting parametrization is $k_{CH_2+H}(T) = (1.69 \pm 0.11) \times 10^{-10} \times (T/298\text{ K})^{(0.05\pm0.010)}$ cm^3 molecule^{-1} s^{-1}, where the errors are 1σ.
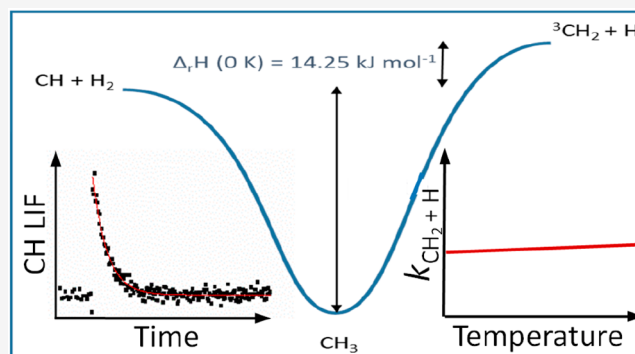
INTRODUCTION

The methylidene radical, CH(X^{2}Π) is a key intermediate in combustion,[1] in reduced atmospheres of planets and moons such as Jupiter and Titan,[2] and in the interstellar medium.[3] The reactivity of CH is such that it can insert into strong bonds, initiating the "prompt" formation of NO$_x$ when reacting with N$_2$[4] and undergoing a number of insertion/elimination reactions with alkanes, alkenes, and alkynes.[5−11] There have been a number of studies of CH kinetics; laser flash photolysis studies have tended to use the multiphoton photolysis of bromoform, CHBr$_3$, to generate CH,[2−9] whereas flow tube studies have used metal atom stripping of Br from CHBr$_3$ to generate CH.[12] Most studies use laser-induced fluorescence at ∼431 nm to probe the CH concentration as a function of time, but chemiluminescence from the CH + O$_2$ reaction has also been used.[13] Given the high endothermicity of CH ($\Delta_f H°$(0 K) = 592.837 ± 0.097 kJ mol^{-1}),[14] many CH reactions have multiple product channels, and several groups have determined quantitative product yields for key CH reactions.[6,10,15]

An important reaction of CH in combustion and in the atmospheres of the giant planets is the reaction with H$_2$ (reaction 1):[16−20]

$$CH + H_2 \rightleftarrows CH_2 + H \qquad (\pm 1)$$

The CH + H$_2$ reaction is thought to proceed via an insertion forming chemically activated methyl radicals, CH$_3$*, that can either be stabilized or eliminate a hydrogen atom to form ground-state methylene, ^{3}CH$_2$, as the coproduct:

$$CH + H_2 \rightarrow CH_3^* \rightarrow {}^3CH_2 + H$$
$$+$$
$$M$$
$$\downarrow$$
$$CH_3$$
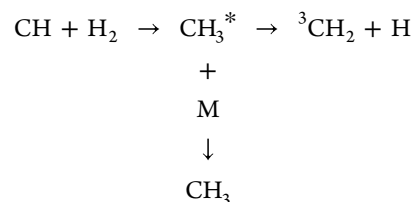
The thermodynamics of the system is well-established, and the potential energy surface (PES) has been calculated by a
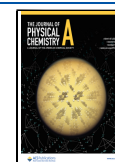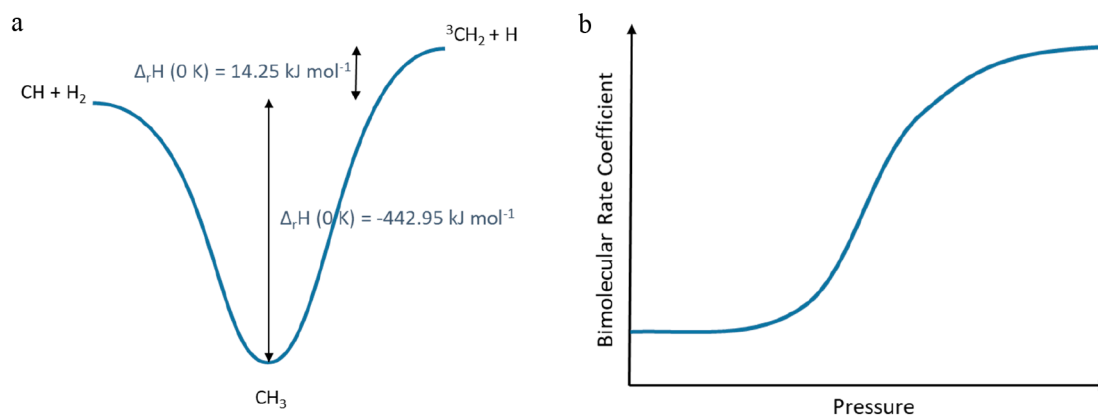
Figure 1. (a) Schematic potential energy surface for reaction 1. Values for $\Delta_r H(0\ K)$ were taken from the Active Thermochemical Tables (ATcT).[14] (b) Schematic showing the expected pressure dependence of reaction 1. At low pressure a limiting value is obtained corresponding to the formation of $^3CH_2 + H$. As the pressure increases, stabilization into the methyl well enhances the rate coefficient.

Table 1. Summary of Previous Kinetics Studies on the $^3CH_2 + H$ Reaction

authors, year	temperature range/K	pressure range	k_{300K}/cm^3 molecule^{-1} s^{-1}	$k(T)/cm^3$ molecule^{-1} s^{-1}	method
Fulle and Hippler, 1997[20]	185–800	1–160 bar	2.2×10^{-10}	$(2.19 \times 10^{-10})(T/298)^{0.32}$	application of equilibrium to studies of the reverse reaction
Rohrig et al., 1997[23]	2200–2600	1 bar		2.34×10^{-10}	indirect measurement from shock tube study of CH + O$_2$
Devriendt et al., 1995[24]	300–1000	2 Torr	4.9×10^{-10}	$5.2 \times 10^{-11} \exp(5610/RT)$	mass spectrometry: rate coefficient measured relative to CH$_2$ + O
Boullart and Peeters, 1992[25]	300	2 Torr	2.7×10^{-10}	n.a.	mass spectrometry: rate coefficient measured relative to CH$_2$ + O
Bohland et al., 1987[26]	298	1–1.6 Torr	1.83×10^{-10}	n.a.	discharge flow, $^3CH_2$ monitored with laser magnetic resonance
Zabernack et al., 1986[27]	300–700		1.4×10^{-10}	$4.7 \times 10^{-10} \exp(-3080/RT)$	application of equilibrium to studies of the reverse reaction

number of groups (see, e.g., refs 21 and 22). A schematic of the PES is shown in Figure 1a. The kinetics of the CH + H$_2$ reaction is expected to show an S-shaped pressure dependence, as shown in Figure 1b; at low pressures no CH$_3$* is stabilized, and the loss of CH is determined by the competition between the forward and backward unimolecular decompositions of CH$_3$*. As the pressure increases, CH$_3$* will start to be stabilized into the CH$_3$ well, and the overall rate coefficient will increase with pressure until it reaches a limit where stabilization outcompetes redissociation. This high-pressure rate coefficient reflects the rate coefficient for CH$_3$* formation.

Reaction 1 was extensively studied by Brownsword et al.[16] At low temperatures, the system behaved as expected, but at the highest temperatures of the study (584 and 744 K) a negative pressure dependence was observed at lower pressures (5–100 Torr). Brownsword et al. suggested that at high temperatures, where a majority of the reagent population is above the threshold to form $^3CH_2 + H$ and hence a majority of CH$_3$* is also above this threshold, collisional deactivation could bring a significant proportion of energized CH$_3$* below the threshold for $^3CH_2 + H$ but above the CH + H$_2$ asymptote, promoting re-formation of reagents and reducing the rate coefficient as a function of pressure. As the pressure increases further, stabilization to CH$_3$ dominates, and the rate coefficient reverts to the expected behavior, increasing with pressure.

The well-known thermodynamics of the system means that the kinetics of the reverse reaction, $^3CH_2 + H$ (reaction −1), can be determined from studies on CH + H$_2$ kinetics. In contrast to the relatively straightforward way that the forward

reaction can be studied (at least at lower temperatures), the reverse reaction is experimentally challenging, requiring the generation of two radical species. If the reaction is carried out under pseudo-first-order conditions ([H] ≫ [$^3CH_2$]), the absolute concentration of hydrogen atoms needs to be known; for second-order kinetics, both radical concentrations need to be known. $^3CH_2$ is also not that easy to detect, with most studies using laser magnetic resonance (LMR) or mass spectrometry. These challenges are reflected in the reported values for k_{-1} summarized in Table 1.

Although $^3CH_2$ has a very high enthalpy of formation ($\Delta_f H°(0\ K) = 391.054 \pm 0.096$ kJ mol^{-1}),[14,28] it is relatively unreactive and much less reactive than the first excited state, $^1CH_2$, which is only 37.66 kJ mol^{-1} higher in energy, not undergoing any of the insertion/elimination reactions that characterize $^1CH_2$ chemistry (see, e.g., ref 29). The reaction of $^3CH_2$ with H is a notable exception in terms of reactivity, and although there is a wide variation in the magnitude of k_{-1} and even some uncertainty in the direction of its temperature dependence, the rate coefficient is relatively high (~0.8[30] to 5[24] × 10^{-10} cm^3 molecule^{-1} s^{-1}). Hence in environments with high [H] such as flames[31,32] and the upper regions of the atmospheres of the giant planets,[33] reaction −1 can convert relatively unreactive $^3CH_2$ into reactive CH species. For combustion chemistry, both Hughes et al.[31] and Glarborg et al.[32] highlighted the important role of reaction −1, the scatter of the current literature data, and the need for further studies.

In this paper we present new experimental data on the reaction of CH + H$_2$ with a particular focus on resolving the
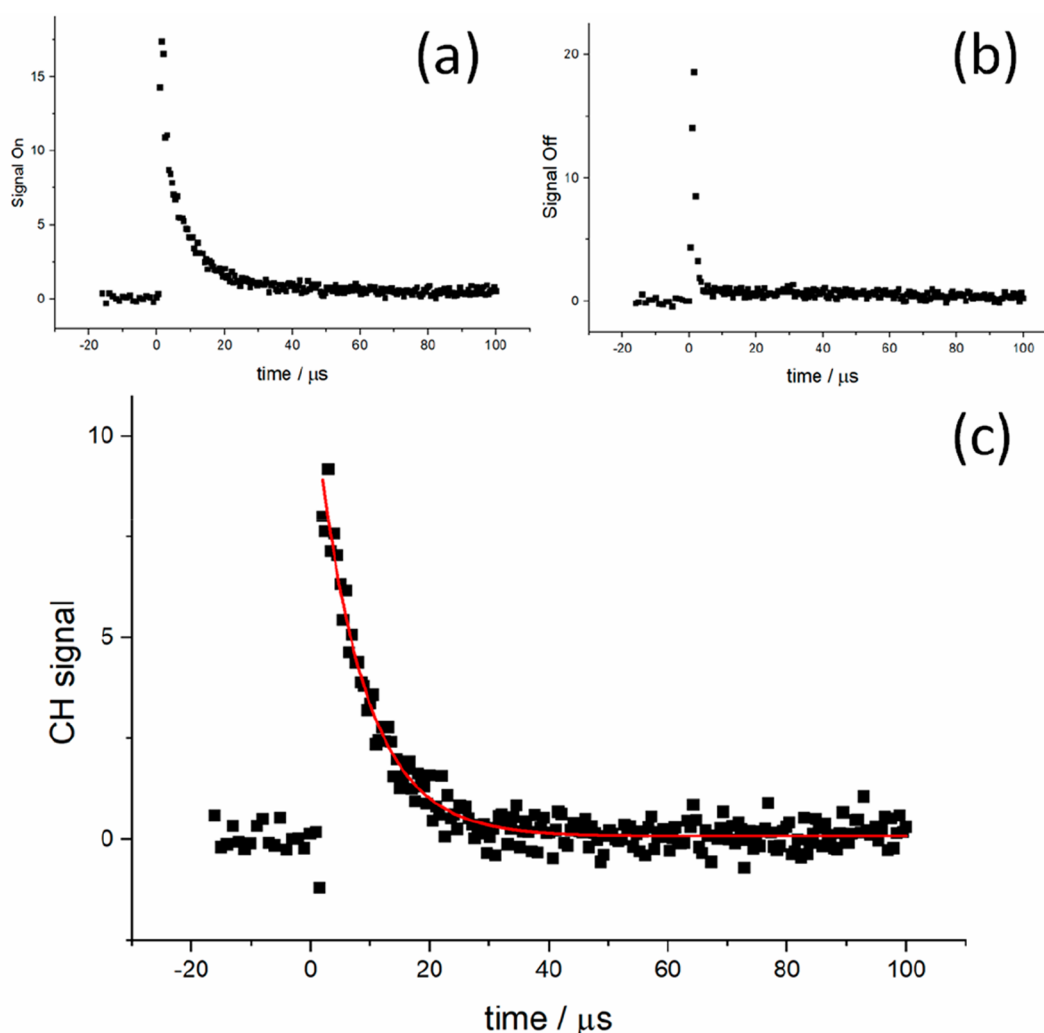
Figure 2. Elimination of interference. (a) Total signal recorded at ~428 nm ($R_1(4)$ line), CH and background signal. (b) Signal recorded with the dye laser moved 0.17 nm, i.e., off the $R_1(4)$ CH line but with a very similar background signal. (c) Subtraction of the two traces yields the CH-only signal. The red line is an exponential fit to the data.

abnormal pressure dependence at high temperatures and low pressures. We then combine our data with literature measurements on reaction 1 and test the dataset for consistency using the master equation program MESMER.[34−36] Given the well-defined thermochemistry for reactions 1 and −1, precise predictions of k_{-1} based on the consensus data of k_1 can be made.

■ METHODS

Experimental Section. Reaction 1 was studied in a conventional slow-flow laser flash photolysis system with time-resolved detection of CH by laser-induced fluorescence (LIF) under pseudo-first-order conditions. Details on previous studies can be found in McKee et al.[6] and Blitz et al.[15,37] The CH precursor, bromoform (Sigma-Aldrich, 98% purity) was stored as dilute mixtures (argon) in glass bulbs and metered using calibrated mass flow controllers. Precursor gas mixtures, H_2 (BOC, >99.99%), and argon bath gas were combined in a mixing manifold and flowed through a metal reaction cell. Additionally, a few experiments were carried out with helium as the bath gas. Temperatures were recorded with calibrated thermocouples, and pressures in the cell were determined via capacitance manometers.

Bromoform was photolyzed by an excimer laser at 248 nm. CH production occurs via a multiphoton absorption process, and several other species such as H and $CHBr_x$ will be formed in the photolysis:

$$CHBr_3 \xrightarrow{nh\nu} CH, \ H, \ CHBr_x \tag{2}$$
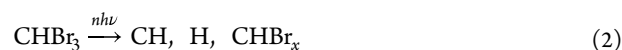
Typical excimer fluences were 50 mJ cm^{-2} $pulse^{-1}$, and the excimer laser was operated at 10 Hz, which was sufficient for replenishment of a fresh gas mix for each laser shot.

CH was probed via LIF at 428 nm (the $R_1(4)$ line of the A ← X transition) generated from a YAG (Quantel 850, 355 nm, 10 Hz)-pumped dye laser (Sirah, operating on Stilbene 420 dye), and resonant fluorescence was observed perpendicular to the axes of both the photolysis and probe lasers with a microchannel plate photomultiplier. The time delay between the photolysis and probe pulses was varied in order to build up a decay curve.

At close to time zero, CH* emission was observed that is a result of the multiphoton dissociation of $CHBr_3$. In addition, as the temperature was increased a structureless spectrum was observed between 425−440 nm, possibly due to LIF from a $CHBr_x$ species. This emission swamps the strong CH LIF line

at 431 nm that is normally used to monitor CH but has less impact on the $R_1(4)$ line at 428 nm. We experimented with a narrow-band filter $(430 \pm 5\ nm)$, but this had limited effect, as it passed a significant amount of both the CH* emission and the background LIF. In order to account for both the spontaneous fluorescence from CH* and LIF from the unknown species, two decay traces were recorded for each condition, first with the probe laser tuned to the peak of the $R_1(4)$ line (recording emission from CH*, CH, and the unknown species) and then with the laser moved by $\sim$0.17 nm, sufficient to move off the $R_1(4)$ line, but without any significant change in the LIF signal from the unknown species. Subtraction of the two decay profiles yielded the CH LIF decay. An example of the process is shown in Figure 2.

The system was studied under pseudo-first-order conditions with $[H_2] \gg [CH]_0$. Under these conditions, the resulting CH decay curves should be exponential (as shown in Figure 2c) with the pseudo-first-order rate coefficient, k_{obs}, being given by

$$k_{obs} = k_1[H_2] + k_d \tag{3}$$

where k_1 is the pressure-dependent bimolecular rate coefficient and k_d is an effective first-order rate coefficient that accounts for the reaction of CH with bromoform and diffusion out of the observation region.

Figure 3 shows a typical bimolecular plot of k_{obs} versus $[H_2]$, the gradient of which is k_1. Experiments were repeated for a
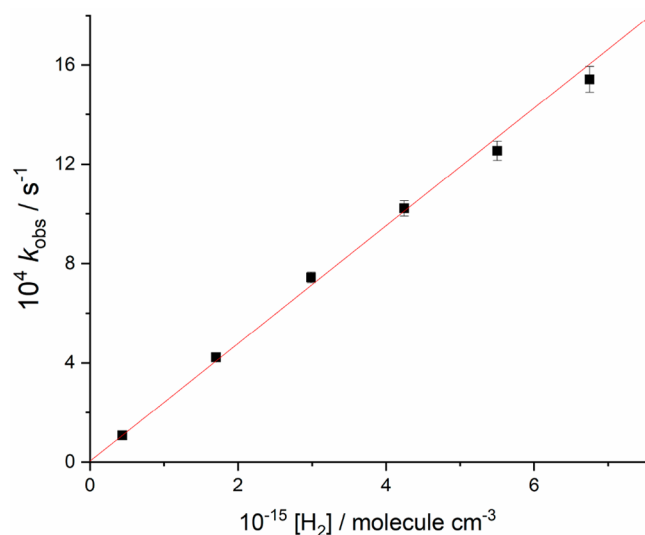
Figure 3. Bimolecular plot at 748 K and 70.3 Torr total pressure of argon. A weighted linear fit to the data gives $k_1 = (2.37 \pm 0.05) \times 10^{-11}\ cm^3\ molecule^{-1}\ s^{-1}$, where the error reported is the statistical error at the 1σ level.

range of pressures at each temperature, and checks were made to ensure the invariance of the rate coefficients with photolysis laser energy or repetition rate. Figure 4 shows the dependence of k_1 as a function of pressure at $\sim$744 K. The data are tabulated in Table S1. The errors reported for the bimolecular rate coefficients in this article are the statistical errors at the 1σ level from the bimolecular plots. We suggest that these errors should be combined with an estimated 10% systematic error to give the overall error. These errors are reported in Table S1.

MESMER Analysis. The master equation program MESMER was used to analyze the data obtained in this study and some literature data. Details on the MESMER
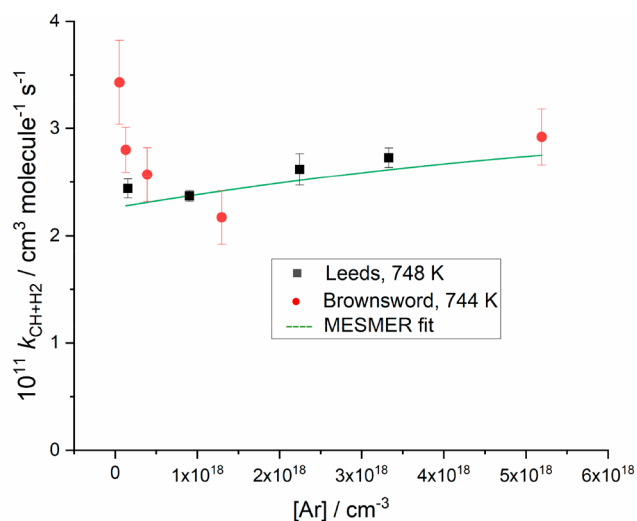
Figure 4. Example of the pressure dependence of k_1 recorded at the temperature of $\sim$744 K. The figure shows data from this work (black ■) and Brownsword et al.[16] (red ●).

program can be found in ref 34, and applications to analysis of literature data can be found in refs 36 and 38. Simulations using MESMER were undertaken to explore whether it was possible to reproduce the observations of Brownsword et al.[16]

MESMER contains a data-fitting routine based on Marquardt least-squares analysis. In the current analysis a variety of parameters were varied. The energy transfer parameter, $\langle \Delta E \rangle_d$ (the average transferred in a downward direction), was assigned a temperature dependence of the form $A(298\ K) \times T^n$, and values of A and n could be set for each bath gas, allowing us to directly compare experiments carried out in He and Ar.

The first data analysis was limited to experimental studies on the CH + H_2 reaction. The datasets used were those from McIlroy and Tully,[39] Fulle and Hippler,[20] Brownsword et al.[16] and Zabarnick et al.[27] A second stage in the analysis was to combine high-temperature shock tube data on CH_3 decomposition. A number of studies have looked at CH_3 decomposition, probing both the loss of CH_3 and product formation. The study by Vasudevan et al.[40] monitored both CH and OH productions in the presence of oxygen. OH production was associated with the conversion of $^3CH_2$ and H to OH via the well-studied reaction of $^3CH_2$ with oxygen[41] and the H + O_2 reaction. However, CH will also react with O_2 to generate OH, so OH production is not a unique signature of $^3CH_2$ production.

RESULTS AND DISCUSSION

Experimental Studies on the Reaction of CH with H_2. Figure 4 shows an example of the pressure-dependent bimolecular rate coefficients. In their work, Brownsword et al.[16] had observed significant *decreases* in the bimolecular rate coefficient k_1 with pressure at low pressures (e.g., $(3.43 \pm 0.39) \times 10^{-11}\ cm^3\ molecule^{-1}\ s^{-1}$ to $(2.17 \pm 0.25) \times 10^{-11}\ cm^3\ molecule^{-1}\ s^{-1}$ from 4 to 100 Torr at 744 K; red points in Figure 4). Brownsword et al. carefully considered possible errors and uncertainties in their experiments but concluded that the effects were real. They suggested that a negative pressure effect could occur at high temperatures, where initial collisions could reduce the energy of CH_3* below the exit

Table 2. Fitting Parameters for the CH + H_2/CH_3/$^3CH_2$ + H System (Reported Errors Are 1σ)

parameter	fit 1: CH + H_2 data only; $\Delta_rH_1(0\ K)$ floated	fit 2: CH + H_2 $\Delta_rH_1(0\ K)$ fixed to ATcT value	fit 3: CH + H_2 and selected CH_3 data; $\Delta_rH_1(0\ K)$ fixed to ATcT value	fit 4: CH + H_2 and selected CH_3 data; extended T dependence of $\langle\Delta E\rangle_d(T)$
$A_{\langle\Delta E\rangle_d}$ (Ar)/cm^{-1}	42.3 ± 5.6	48.9 ± 2.5	50.6 ± 2.6	54.8 ± 2.9
$A_{\langle\Delta E\rangle_d}$ (He)/cm^{-1}	28.0 ± 4.6	34.5 ± 1.2	34.7 ± 1.3	35.1 ± 1.3
n (Ar)	1.15 ± 0.16	1.11 ± 0.13	1.017 ± 0.025	1.45 ± 0.12
n (He)	1.38 ± 0.27	1.31 ± 0.11	1.30 ± 0.12	1.32 ± 0.12
B (Ar)/K^{-1}	n/a	n/a	n/a	$(3.6 \pm 1.0) \times 10^{-4}$
A_{CH+H_2}/cm^3 s^{-1}	$(3.49 \pm 0.47) \times 10^{-10}$	$(2.57 \pm 0.24) \times 10^{-10}$	$(2.71 \pm 0.27) \times 10^{-10}$	$(2.63 \pm 0.26) \times 10^{-10}$
$n^\infty_{CH+H_2}$	−0.30 ± 0.44	0.15 ± 0.19	0.23 ± 0.20	0.22 ± 0.19
A_{CH_2+H}/cm^3 s^{-1}	$(2.3 \pm 4.4) \times 10^{-10}$	$(1.71 \pm 0.11) \times 10^{-10}$	$(1.75 \pm 0.11) \times 10^{-10}$	$(1.69 \pm 0.11) \times 10^{-10}$
$n^\infty_{CH_2+H}$	−0.05 ± 1.5	0.08 ± 0.11	0.03 ± 0.10	0.05 ± 0.10
$\Delta_rH_1(0\ K)$/kJ mol^{-1}	14.9 ± 5.4	14.25[14]	14.25[14]	14.25[14]
χ^2/degree of freedom	0.86	0.84	1.16	0.73

channel for $^3CH_2$ + H but still allowing redissociation to reagents and called for further investigations via a master equation approach.

We do not see a negative dependence with pressure over a similar pressure regime to that studied by Brownsword et al. (although they did go to slightly lower pressures), but there are some hints of unusual behavior at our very lowest pressures. We believe that this could be due to nonthermal ro-vibrational distributions in the photolytically produced CH. We carried out a range of calculations using MESMER but could not simulate any negative pressure effects even though we explored a wide range of conditions. Additionally, we constructed a three-state methyl model based on the hypothesis of Brownsword et al. considering CH_3** (enough energy to form $^3CH_2$ + H), CH_3* (enough energy to dissociate back to reagents), and stabilized CH_3. Using this model, it is indeed possible to simulate the behavior observed by Brownsword et al., but only if unrealistic parameters which cannot be included in a master equation approach (e.g., redissociation to reagents is slower for CH_3** than CH_3*) are used. Further details are given in section 2 of the Supporting Information. We suggest that the unusual behavior observed by Brownsword et al. is due to the prompt fluorescence or rotational relaxation not being fully accounted for, but there may be other possible explanations.

In general our data on reaction 1 are in good agreement with previous work: we observe the same trends of a positive temperature dependence in k_1 at low pressure associated with the positive enthalpy of reaction to form $^3CH_2$ + H and a positive pressure dependence at a fixed temperature as more CH_3* is stabilized. A quantitative comparison with the existing literature is presented in the next section.

MESMER Analysis. Our initial fits were based solely on the CH + H_2 datasets. First, we fitted the data floating both the thermochemistry of reaction 1 and the energy transfer parameters. The resulting fits to the CH + H_2 were reasonable (errors are 1σ), but the thermochemistry of the reaction, while in agreement with the literature, was not well-defined (Fit 1 in Table 2); hence, there are corresponding uncertainties in the kinetic parameters for reaction −1. An equally good fit, but with precise data on the kinetics of reaction −1, can be obtained by constraining the thermochemistry of reaction 1 to the values presented in ATcT. The parameters for this fit are shown as Fit 2 in Table 2. The reaction enthalpy in ATcT is $\Delta_rH°(0\ K) = 14.25 \pm 0.11$ kJ mol^{-1},[14,28,42] where the error comes from the full covariance matrix at the 95% confidence

limit. The individual uncertainties for CH and $^3CH_2$ are low (~0.1 kJ mol^{-1}), and the recommended value is based on a wide range of provenance.

The energy transfer parameters for argon and helium are well-defined and are comparable with data from similar systems.[32] As with other fits, $\langle\Delta E\rangle_d$, the average energy transferred in a downward direction, shows a positive temperature dependence, scaling in an almost linear fashion with temperature over the range 185−800 K. However, when high-temperature shock tube data are included, $\langle\Delta E\rangle_d$ shows a more complex temperature dependence as discussed below.

We also included experimental data from Vasudevan et al.,[40] who monitored the decomposition of CH_3 via shock tube methods with direct detection of CH but also reported significant production of $^3CH_2$ + H via direct observation of OH, which was considered as a proxy for $^3CH_2$ + H. We are able to include the CH data in the MESMER analysis with good quality fits (Fit 3, Table 2). However, MESMER simulations show that production of the $^3CH_2$ + H channel does not occur to any great extent under the experimental conditions of Vasudevan et al., as shown in Figure 5.

The lower-energy product channel of CH + H_2 versus $^3CH_2$ + H ensures that at the conditions of the shock tube experiments, any CH_3* above threshold exits as CH + H_2
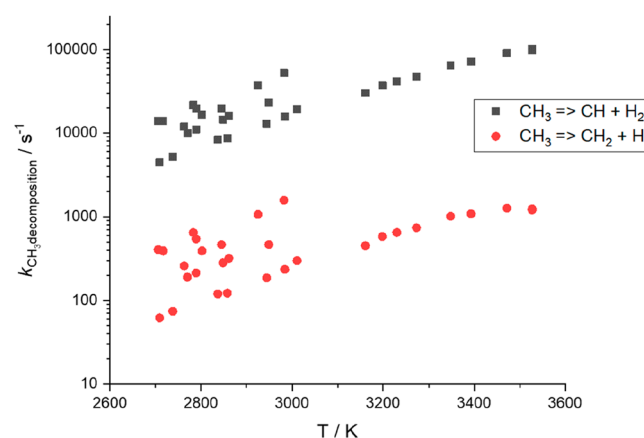
Figure 5. MESMER simulations of the rates of CH_3 decomposition to CH + H_2 (black ■) and $^3CH_2$ + H (red ●) under the conditions used by Vasudevan et al.[40] The reaction is dominated by production of CH and H_2. From 2700−3000 K, multiple points at a given temperature are due to the variation in pressure from 0.7−4.2 bar.

rather than undergoing additional excitation to access the $^3CH_2$ + H product channel. Vasudevan et al. suggested that CH and $^3CH_2$ are formed in roughly equal amounts based on their observations of both CH and OH product. Their assignment of the yield assumed that the observed long-time OH signal could be solely assigned to the $^3CH_2$ + H channel. However, it is known that CH + O_2 as well as $^3CH_2$ + O_2 can lead to OH.[41,43,44]

Qualitatively similar arguments have been presented by Fulle and Hippler.[20] At low pressures all of the activated CH_3^* will dissociate to CH and H_2, but at the high pressure limit, while CH + H_2 will be the dominant channel, approximately 25% of CH_3 will dissociate to $^3CH_2$ + H at ~2000 K. However, the high-pressure limit will only be reached at pressures of several thousand bar, significantly greater than the pressures used by Vasudevan et al. (0.7–4.2 bar).

Figure 6 shows the fit to the datasets on the CH + H_2 and CH_3 decomposition reactions as a function of temperature and pressure. The literature data on CH + H_2 cover the temperature and pressure ranges 185–800 K and 5–76000 Torr, and generally there is excellent agreement across the dataset between the experimental data and the MESMER fit. A similarly good fit is obtained when the direct measurements of CH from CH_3 decomposition are included in Fit 3. The fit to the shock tube data is shown in the lower panel of Figure 6.

One further point to notice here is the function used to fit the energy transfer parameter $\langle \Delta E \rangle_d$ from the complete set of experimental data. A simple $A \times (T/298 \text{ K})^n$ dependence is no longer suitable over this wider temperature range, and the energy transfer parameters at shock tube conditions are overestimated by this simple parametrization. Such effects have been noted in our previous studies on CH_3 recombination.[38] The parametrization of energy transfer by argon has been extended to include an additional temperature dependence to allow for the observed reduction in efficiency at high temperatures:

$$\langle \Delta E \rangle_d = A \left(\frac{T}{298} \right)^n \exp(-B^* T) \tag{4}$$

Incorporating this additional parameter into the fit decreases the reduced χ^2 parameter by approximately 40% from Fit 3 to Fit 4.

The final column of Table 2 shows our best estimates of the fitting parameters. The parameters for the limiting rate coefficients of the bimolecular reactions are well-defined, and the implications are discussed in the next subsection.

Implications for k_{-1}. The recommendation from this work is that the rate coefficient for the reaction $^3CH_2$ + H → CH + H_2 (reaction −1) can be parametrized as $k_{-1}(T) = (1.69 \pm 0.11) \times 10^{-10} \times (T/298 \text{ K})^{(0.05 \pm 0.010)}$ cm^3 molecule^{-1} s^{-1}, where the errors are 1σ. Figure 7 shows the temperature dependence for k_{-1} based on both this work and various literature studies. This work, the theoretical calculations of Garcia et al.,[21] and the recommendations of the Baulch et al.[45] review are in excellent agreement on the lack of any significant temperature dependence, and room-temperature values vary over a relatively narrow range from (1.7 to ~3) × 10^{-10} cm^3 molecule^{-1} s^{-1}. Our result is also in excellent agreement with the room-temperature study of Bohland et al.[26] (1.83 × 10^{-10} cm^3 molecule^{-1} s^{-1}). This good level of agreement is in marked contrast to the conclusions of both the most recent direct study of Devriendt et al.[24] and the earlier calculations
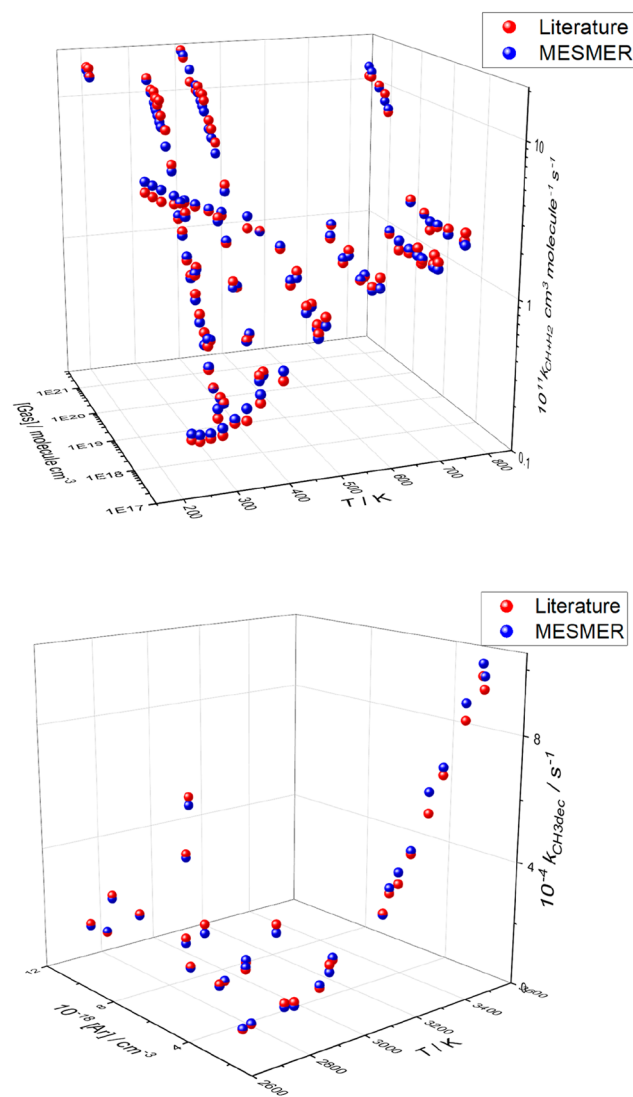
Figure 6. MESMER fit to literature data. The fitting parameters are given in the final column of Table 2. Upper panel: Fit to CH + H_2 data. The low-pressure data at the front of the plot show the increase in k_1 as a function of temperature; here the dominant channel is the formation of $^3CH_2$ + H. The increase in k_1 as a function of pressure can also be seen leading to increasing formation of CH_3. Lower panel: Fit to CH_3 → CH + H_2 shock tube data. Again there is a strong increase with temperature and an increase with pressure, but the data are far from the high-pressure limit.

based on measurements of k_1 and application of equilibrium: $K_1 = k_1/k_{-1}$ from Fulle and Hippler and Zabarnick et al. Given the importance of reaction −1 in converting relatively unreactive $^3CH_2$ to reactive CH radicals, it is important for both combustion and planetary atmosphere modeling that k_{-1} is well-defined.

Direct studies of k_{-1} are challenging. Devriendt et al.[24] generated $^3CH_2$ from the reaction of O atoms with ketene, which efficiently produces $^3CH_2$ but also forms other radicals. CH_2 was monitored by mass spectrometry, but corrections had to be made for a component of the CH_2 signal arising from ketene ionization. Finally, k_{-1} was not measured directly but was measured relative to the reaction of $^3CH_2$ with O, and k_{CH_2+O} was taken to be temperature-independent from a review
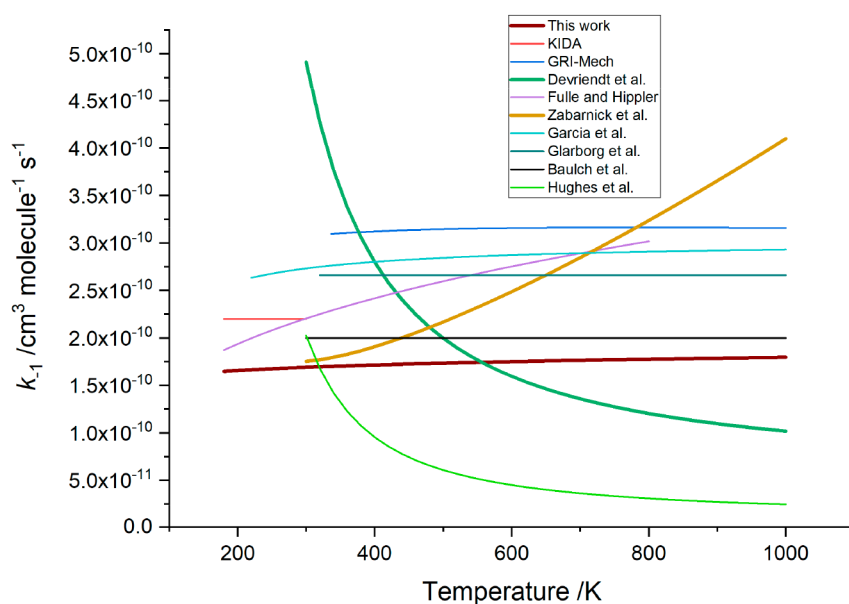
Figure 7. Temperature dependence of selected data on reaction −1, $^3CH_2 + H \rightarrow CH + H_2$. Three traces have been highlighted to show the variation in temperature dependence. Devriendt et al. report a strong negative temperature dependence based on experimental studies where reaction −1 was monitored relative to $^3CH_2 + O$. Zabarnick et al. report a positive temperature dependence based on experimental studies of reaction 1 and application of equilibrium. Finally, this work shows a temperature-independent value for k_{-1} using a similar approach to Zabarnick et al. but with updated thermochemistry.

of the relatively limited literature with a value of 1.3×10^{-10} cm^3 molecule^{-1} s^{-1}. Values close to room temperature, where a majority of the measurements of k_{CH_2+O} have been made, are in reasonable agreement with this work. It may therefore be that the higher-temperature measurements of $^3CH_2 + O$ are in error. Devriendt et al. suggested that their observed negative temperature dependence is in good agreement with shock tube measurements (e.g., Frank et al.,[46] $k_{-1} = 1.3 \times 10^{-11}$ cm^3 molecule^{-1} s^{-1}) and rationalized the decrease in k_{-1} due to the more constrained transition state leading to CH + H$_2$. However, a strong negative temperature dependence for k_{-1} is simply not consistent with the well-determined thermochemistry and kinetics for reaction 1, and other shock tube measurements give considerably higher values (e.g., Rohrig et al.,[23] 2.34×10^{-10} cm^3 molecule^{-1} s^{-1}).

Zabarnick et al.[27] and Fulle and Hippler[20] used a similar analysis to this work to determine k_{-1} based on a calculation via the equilibrium constant. However, in such calculations, the value of the rate coefficient, in this case k_{-1}, is extremely sensitive to the absolute thermochemistry of the reaction and its temperature dependence. In comparison to more recent studies, the temperature dependence of the thermochemistry used by Fulle and Hipplier and Zabarnick et al. was slightly weaker, and hence, the well-defined and significant positive activation energy for k_1 translates to a weak positive temperature dependence for k_{-1}.

The results of this work are in excellent agreement with the review of Baulch et al.,[45] which is the basis of several combustion codes (e.g., Christensen and Konnov, 2017[47]). However, in general a wide range of values for k_{-1} have been used in combustion models. Hughes et al.[31] considered in detail a number of reactions that influence methane chemistry, including reaction −1, and emphasized the important role that the $^3CH_2 + H$ reaction plays in generating reactive CH. The rate expression used, 1×10^{-11} exp(7500 J mol^{-1}/RT) cm^3 molecule^{-1} s^{-1}, is in marked contrast to the recommendation

of this work, in terms of both absolute value under combustion conditions and the temperature dependence: at 1000 K the rate coefficient is close to a factor 10 lower than the recommendation of this work. GRI-Mech 3.0[48] uses a temperature-independent value for k_{-1} that is approximately a factor of 2 higher than that in this work. GRI-Mech is another common base mechanism used in more specialized combustion models. In contrast, while the Aramco mechanism[49] also uses a temperature-independent value for k_{-1}, the value of 5×10^{-11} cm^3 molecule^{-1} s^{-1} for k_{-1} is approximately a factor of 3 less than that recommended in this work. Finally, the role of reaction −1 was also reviewed in the appendix of Glarborg et al.'s work on combustion mechanisms of nitrogen-containing species.[32] Their recommended temperature-independent rate coefficient is $k_{-1} = 2.66 \times 10^{-10}$ cm^3 molecule^{-1} s^{-1}.

Reaction −1 is also important in planetary chemistry: at temperatures of 100−200 K relevant for the upper atmospheres of the outer planets, extrapolations of either the Devriendt et al. data (which would be beyond the temperature range of the experiments) or the Fulle and Hippler data would produce very different rate coefficients. However, many recent models will be based on the data evaluations of the KIDA group,[50] and here the recommended rate coefficient from 10− 298 K is a temperature-independent value of 2.2×10^{-10} cm^3 molecule^{-1} s^{-1}, which is only approximately 30% above the recommendation of this work. Therefore, the impact on chemical models based on KIDA data should not be too great. However, well-cited earlier modeling studies such as the work of Wilson and Atreya[51] or Vuitton et al.[33,52] on benzene formation in Titan use data on k_{-1} from Zabarnick et al. and Fulle and Hippler, respectively, and therefore, changes may be required to account for variations in reactive CH formation.

CONCLUSIONS

New results on the CH + H$_2$ reaction (reaction 1) have been obtained using laser flash photolysis combined with laser-induced detection of CH. Care needs to be taken to avoid interference from other species. In contrast to Brownsword et al.,[16] no anomalous pressure dependence was observed. Our own data and other literature data on reaction 1 and the decomposition kinetics of methyl radicals have been combined and analyzed using a master equation code. The analysis provides a precise determination of the kinetics of the reaction $^3CH_2 + H \rightarrow CH + H_2$ (reaction −1): $k_{-1}(T) = (1.69 \pm 0.11) \times 10^{-10} \times (T/298 \text{ K})^{(0.05\pm0.010)}$ cm^3 molecule^{-1} s^{-1}. The magnitude and temperature dependence of k_{-1} differ significantly from both some experimental data and the values used in some combustion and planetary atmosphere models.

ASSOCIATED CONTENT

Supporting Information

The Supporting Information is available free of charge at https://pubs.acs.org/doi/10.1021/acs.jpca.2c08097.

> Experimental rate coefficients k_1 as a function of temperature and pressure, detailed analysis of the three-state model proposed by Brownsword et al., and an example MESMER input file (PDF)

AUTHOR INFORMATION

Corresponding Authors

Mark A. Blitz − *School of Chemistry and NCAS, University of Leeds, Leeds LS2 9JT, U.K.;* ◎ orcid.org/0000-0001-6710-4021; Email: m.blitz@leeds.ac.uk

Paul W. Seakins − *School of Chemistry, University of Leeds, Leeds LS2 9JT, U.K.;* ◎ orcid.org/0000-0002-4335-8593; Email: p.w.seakins@leeds.ac.uk

Authors

Lavinia Onel − *School of Chemistry, University of Leeds, Leeds LS2 9JT, U.K.*

Struan H. Robertson − *Dassault Systemes, Cambridge CB2 0WN, U.K.*

Complete contact information is available at:
https://pubs.acs.org/10.1021/acs.jpca.2c08097

Notes

The authors declare no competing financial interest.

ACKNOWLEDGMENTS

REFERENCES

(1) Pilling, M. J. From elementary reactions to evaluated chemical mechanisms for combustion models. *Proc. Int. Symp. Combust.* **2009**, *32*, 27−44.

(2) Blitz, M. A.; Seakins, P. W. Laboratory studies of photochemistry and gas phase radical reaction kinetics relevant to planetary atmospheres. *Chem. Soc. Rev.* **2012**, *41* (19), 6318−6347.

(3) Jacob, A. M.; Menten, K. M.; Gong, Y.; Bergman, P.; Tiwari, M.; Brünken, S.; Olofsson, A. O. H. Hunting for the elusive methylene radical. *Astron. Astrophys.* **2021**, *647*, A42.

(4) Medhurst, L. J.; Garland, N. L.; Nelson, H. H. CH + N$_2$ = HCN$_2$ kinetic-study of the addition channel from 300 to 1100 K. *J. Phys. Chem.* **1993**, *97* (47), 12275−12281.

(5) Blitz, M. A.; Johnson, D. G.; Pesa, M.; Pilling, M. J.; Robertson, S. H.; Seakins, P. W. Reaction of CH radicals with methane isotopomers. *J. Chem. Soc., Faraday Trans.* **1997**, *93* (8), 1473−1479.

(6) McKee, K.; Blitz, M. A.; Hughes, K. J.; Pilling, M. J.; Qian, H. B.; Taylor, A.; Seakins, P. W. H atom branching ratios from the reactions of CH with C$_2$H$_2$, C$_2$H$_4$, C$_2$H$_6$, and neo-C$_5$H$_{12}$ at room temperature and 25 Torr. *J. Phys. Chem. A* **2003**, *107* (30), 5710−5716.

(7) Thiesemann, H.; Clifford, E. P.; Taatjes, C. A.; Klippenstein, S. J. Temperature dependence and deuterium kinetic isotope effects in the CH(CD) + C$_2$H$_4$(C$_2$D$_4$) reaction between 295 and 726 K. *J. Phys. Chem. A* **2001**, *105* (22), 5393−5401.

(8) Thiesemann, H.; MacNamara, J.; Taatjes, C. A. Deuterium kinetic isotope effect and temperature dependence in the reactions of CH $^2\Pi$ with methane and acetylene. *J. Phys. Chem. A* **1997**, *101* (10), 1881−1886.

(9) Loison, J. C.; Bergeat, A. Rate constants and the H atom branching ratio of the reactions of the methylidyne CH(X $^2\Pi$) radical with C$_2$H$_2$, C$_2$H$_4$, C$_3$H$_4$ (methylacetylene and allene), C$_3$H$_6$ (propene) and C$_4$H$_8$ (*trans*-butene). *Phys. Chem. Chem. Phys.* **2009**, *11* (4), 655−664.

(10) Loison, J. C.; Bergeat, A.; Caralp, F.; Hannachi, Y. Rate constants and H atom branching ratios of the gas-phase reactions of methylidyne CH radical with a series of alkanes. *J. Phys. Chem. A* **2006**, *110* (50), 13500−13506.

(11) Berman, M. R.; Lin, M. C. Kinetics and mechanisms of the reactions of CH with CH$_4$, C$_2$H$_6$ and n-C$_4$H$_{10}$. *Chem. Phys.* **1983**, *82* (3), 435−442.

(12) Anderson, S. M.; Freedman, A.; Kolb, C. E. Fast-flow studies of CH radical kinetics at 290 K. *J. Phys. Chem.* **1987**, *91* (24), 6272−6277.

(13) Carl, S. A.; Van Poppel, M.; Peeters, J. Identification of the CH + O$_2$ → OH(A) + CO reaction as the source of OH(A−X) chemiluminescence in C$_2$H$_2$/O/H/O$_2$ atomic flames and determination of its absolute rate constant over the range T = 296 to 511 K. *J. Phys. Chem. A* **2003**, *107* (50), 11001−11007.

(14) Ruscic, B.; Pinzon, R. E.; Morton, M. L.; von Laszevski, G.; Bittner, S. J.; Nijsure, S. G.; Amin, K. A.; Minkoff, M.; Wagner, A. F. Introduction to active thermochemical tables: Several "key" enthalpies of formation revisited. *J. Phys. Chem. A* **2004**, *108* (45), 9979−9997.

(15) Blitz, M. A.; Talbi, D.; Seakins, P. W.; Smith, I. W. M. Rate constants and branching ratios for the reaction of CH radicals with NH$_3$: A combined experimental and theoretical study. *J. Phys. Chem. A* **2012**, *116* (24), 5877−5885.

(16) Brownsword, R. A.; Canosa, A.; Rowe, B. R.; Sims, I. R.; Smith, I. W. M.; Stewart, D. W. A.; Symonds, A. C.; Travers, D. Kinetics over a wide range of temperature (13−744 K): Rate constants for the reactions of CH(*v* = 0) with H$_2$ and D$_2$ and for the removal of CH(*v* = 1) by H$_2$ and D$_2$. *J. Chem. Phys.* **1997**, *106* (18), 7662−7677.

(17) Berman, M. R.; Lin, M. C. Kinetics and mechanisms of the reactions of CH and CD with H$_2$ and D$_2$. *J. Chem. Phys.* **1984**, *81* (12), 5743−5752.

(18) Becker, K. H.; Engelhardt, B.; Wiesen, P.; Bayes, K. D. Rate constants for CH(X$^2\Pi$) reactions at low total pressures. *Chem. Phys. Lett.* **1989**, *154* (4), 342−348.

(19) McIlroy, A.; Tully, F. P. CH+H$_2$ reaction-kinetics - temperature and pressure-dependence and Rice-Ramsperger-Kassel-Marcus master equation calculation. *J. Chem. Phys.* **1993**, *99* (5), 3597−3603.

(20) Fulle, D.; Hippler, H. The temperature and pressure dependence of the reaction CH + H$_2$ = CH$_3$ = CH$_2$ + H. *J. Chem. Phys.* **1997**, *106* (21), 8691−8698.

(21) Garcia, E.; Jambrina, P. G.; Lagana, A. Kinetics of the H + CH$_2$ → CH + H$_2$ Reaction at Low Temperature. *J. Phys. Chem. A* **2019**, *123* (34), 7408−7419.

(22) Aoyagi, M.; Shepard, R.; Wagner, A. F. An ab initio theoretical-study of the CH + H$_2$ = CH$_3$* = CH$_2$ + H reactions. *Int. J. Supercomput. Appl. High Perform. Comput.* **1991**, *5* (1), 72−89.

(23) Rohrig, M.; Petersen, E. L.; Davidson, D. F.; Hanson, R. K.; Bowman, C. T. Measurement of the rate coefficient of the reaction

CH + O$_2$ → products in the temperature range 2200 to 2600 K. *Int. J. Chem. Kinet.* **1997**, *29* (10), 781−789.

(24) Devriendt, K.; Vanpoppel, M.; Boullart, W.; Peeters, J. Kinetic investigation of the CH$_2$(X ^{3}B$_1$) + H → CH(X ^{2}Π) + H$_2$ reaction in the temperature-range 400 - 1000 K. *J. Phys. Chem.* **1995**, *99* (46), 16953−16959.

(25) Boullart, W.; Peeters, J. Product distributions of the C$_2$H$_2$ + O and HCCO + H Reactions - Rate-Constant of CH$_2$(X ^{3}B$_1$) + H. *J. Phys. Chem.* **1992**, *96* (24), 9810−9816.

(26) Bohland, T.; Temps, F.; Wagner, H. G. A direct study of the reactions of CH$_2$(X ^{3}B$_1$) radicals with H and D atoms. *J. Phys. Chem.* **1987**, *91* (5), 1205−1209.

(27) Zabarnick, S.; Fleming, J. W.; Lin, M. C. Kinetic study of the reaction CH(X^{2}Π)+H$_2$ = CH$_2$(X^{3}B$_1$)+H in the temperature range 372 to 675 K. *J. Chem. Phys.* **1986**, *85* (8), 4373−4376.

(28) Ruscic, B.; Bross, D. H. Active Thermochemical Tables: the thermophysical and thermochemical properties of methyl, CH$_3$, and methylene, CH$_2$, corrected for nonrigid rotor and anharmonic oscillator effects. *Mol. Phys.* **2021**, *119* (21−22), e1969046.

(29) Gannon, K. L.; Blitz, M. A.; Liang, C. H.; Pilling, M. J.; Seakins, P. W.; Glowacki, D. R.; Harvey, J. N. An experimental and theoretical investigation of the competition between chemical reaction and relaxation for the reactions of ^{1}CH$_2$ with acetylene and ethene: implications for the chemistry of the giant planets. *Faraday Discuss.* **2010**, *147*, 173−188.

(30) Homann, K. H.; Wellmann, C. Kinetics and mechanism of hydrocarbon formation in the system C$_2$H$_2$/O/H at temperatures up to 1300 K. *Ber. Bunsen-Ges. Phys. Chem.* **1983**, *87* (7), 609−616.

(31) Hughes, K. J.; Turanyi, T.; Clague, A. R.; Pilling, M. J. Development and testing of a comprehensive chemical mechanism for the oxidation of methane. *Int. J. Chem. Kinet.* **2001**, *33* (9), 513−538.

(32) Glarborg, P.; Miller, J. A.; Ruscic, B.; Klippenstein, S. J. Modeling nitrogen chemistry in combustion. *Prog. Energy Combust. Sci.* **2018**, *67*, 31−68.

(33) Vuitton, V.; Yelle, R. V.; Klippenstein, S. J.; Horst, S. M.; Lavvas, P. Simulating the density of organic species in the atmosphere of Titan with a coupled ion-neutral photochemical model. *Icarus* **2019**, *324*, 120−197.

(34) Glowacki, D. R.; Liang, C. H.; Morley, C.; Pilling, M. J.; Robertson, S. H. MESMER: An open-source master equation solver for multi-energy well reactions. *J. Phys. Chem. A* **2012**, *116* (38), 9545−9560.

(35) Medeiros, D. J.; Robertson, S. H.; Blitz, M. A.; Seakins, P. W. Direct Trace Fitting of Experimental Data Using the Master Equation: Testing Theory and Experiments on the OH + C$_2$H$_4$ Reaction. *J. Phys. Chem. A* **2020**, *124* (20), 4015−4024.

(36) Blitz, M. A.; Pilling, M. J.; Robertson, S. H.; Seakins, P. W.; Speak, T. H. Global Master Equation Analysis of Rate Data for the Reaction C$_2$H$_4$ + H ⇌ C$_2$H$_5$: $\Delta_f H_0^{\ominus}$ C$_2$H$_5$. *J. Phys. Chem. A* **2021**, *125*, 9548−9565.

(37) Blitz, M. A.; Pesa, M.; Pilling, M. J.; Seakins, P. W. Vibrational relaxation of the CH(D)(X^2 Π, v = 1, 2) radical by helium and argon: evidence for a curve crossing mechanism. *Chem. Phys. Lett.* **2000**, *322* (3−4), 280−286.

(38) Blitz, M. A.; Green, N. J. B.; Shannon, R. J.; Pilling, M. J.; Seakins, P. W.; Western, C. M.; Robertson, S. H. Reanalysis of Rate Data for the Reaction CH$_3$ + CH$_3$ → C$_2$H$_6$ Using Revised Cross Sections and a Linearized Second-Order Master Equation. *J. Phys. Chem. A* **2015**, *119* (28), 7668−7682.

(39) McIlroy, A.; Tully, F. P. CH + H$_2$ Reaction-kinetics - temperature and pressure-dependence and RRKM master-equation calculation. *J. Chem. Phys.* **1993**, *99* (5), 3597−3603.

(40) Vasudevan, V.; Hanson, R. K.; Golden, D. M.; Bowman, C. T.; Davidson, D. F. High-temperature shock tube measurements of methyl radical decomposition. *J. Phys. Chem. A* **2007**, *111* (19), 4062−4072.

(41) Blitz, M. A.; Kappler, C.; Pilling, M. J.; Seakins, P. W. ^{3}CH$_2$ + O$_2$: Kinetics and Product Channel Branching Ratios. *Z. Phys. Chem.* **2011**, *225* (9−10), 957−967.

(42) Ruscic, B.; Bross, D. H. ATcT Enthalpies of Formation Based on Version 1.124 of the Thermochemical Network. https://atct.anl. gov/Thermochemical%20Data/version%201.124/index.php (accessed 2022-11-01).

(43) Bergeat, A.; Calvo, T.; Caralp, F.; Fillion, J. H.; Dorthe, G.; Loison, J. C. Determination of the CH+O$_2$ product channels. *Faraday Discuss.* **2001**, *119*, 67−77.

(44) Blitz, M. A.; McKee, K. W.; Pilling, M. J.; Seakins, P. W. Evidence for the dominance of collision-induced intersystem crossing in collisions of ^{1}CH$_2$ with O$_2$. *Chem. Phys. Lett.* **2003**, *372*, 295−299.

(45) Baulch, D. L.; Bowman, C. T.; Cobos, C. J.; Cox, R. A.; Just, T.; Kerr, J. A.; Pilling, M. J.; Stocker, D.; Troe, J.; Tsang, W.; et al. Evaluated Kinetic Data for Combustion Modeling: Supplement II. *J. Phys. Chem. Ref. Data* **2005**, *34* (3), 757−1397.

(46) Frank, P.; Bhaskaran, K. A.; Just, T. High-temperature reactions of triplet methylene and ketene with radicals. *J. Phys. Chem.* **1986**, *90* (10), 2226−2231.

(47) Christensen, M.; Konnov, A. A. Laminar burning velocity of diacetyl plus air flames. Further assessment of combustion chemistry of ketene. *Combust. Flame* **2017**, *178*, 97−110.

(48) Smith, G. P.; Golden, D. M.; Frenklach, M.; Moriarty, N. W.; Eiteneer, B.; Goldenberg, M.; Bowman, C. T.; Hanson, R. K.; Song, S.; Gardiner, W. C., Jr.; et al. *GRI-Mech 3.0.* http://combustion. berkeley.edu/gri-mech/version30/text30.html (accessed 2022-11-01).

(49) Li, Y.; Zhou, C. W.; Somers, K. P.; Zhang, K. W.; Curran, H. J. The oxidation of 2-butene: A high pressure ignition delay, kinetic modeling study and reactivity comparison with isobutene and 1-butene. *Proc. Combust. Inst.* **2017**, *36* (1), 403−411.

(50) Wakelam, V.; Loison, J.-C.; Herbst, E.; Pavone, B.; Bergeat, A.; Béroff, K.; Chabot, M.; Faure, A.; Galli, D.; Geppert, W. D.; et al. The 2014 KIDA network for interstellar chemistry. *Astrophys. J. Suppl. Ser.* **2015**, *217* (2), 20.

(51) Wilson, E. H.; Atreya, S. K. Current state of modeling the photochemistry of Titan's mutually dependent atmosphere and ionosphere. *J. Geophys. Res.: Planets* **2004**, *109* (E6), E06002.

(52) Vuitton, V.; Doussin, J. F.; Benilan, Y.; Raulin, F.; Gazeau, M. C. Experimental and theoretical study of hydrocarbon photochemistry applied to Titan stratosphere. *Icarus* **2006**, *185* (1), 287−300.